Anisotropic surface acoustic wave scattering in quantum-wire arrays

G. R. Nash and S. J. Bending
School of Physics, University of Bath, Bath BA2 7AY, United Kingdom

M. Boero
Department of Physics, University of Exeter, Exeter EX4 4QL, United Kingdom

P. Grambow, K. Eberl, and Y. Kershaw
Max-Planck-Institut für Festkörperforschung, D-70569 Stuttgart, Germany

(Received 3 June 1996)

We have investigated anisotropic surface-acoustic-wave (SAW) scattering from quantum-wire arrays as a function of electron concentration and magnetic field. With the SAW's propagating perpendicular to the wires, when one naively expects *no* interaction classically, we observe strong oscillations in the transmitted intensity reflecting the magnetic depopulation of one-dimensional subbands as described by a full quantum-mechanical description of the SAW-electron interaction. With the SAW parallel to the wires we observe suppression of SAW-electron scattering rates at low electron concentrations in narrow wires as predicted on the basis of phase-space arguments. Surprisingly, at high electron concentrations, the SAW attenuation increases sharply to where it is three times larger than the maximum possible in the unstructured two-dimensional electron gas. We speculate that this could possibly be due to the excitation of intraband two-dimensional plasmonlike modes. [S0163-1829(96)51536-5]

It has long been recognized[1] that semiconductor quantum wires could form the basis of very high mobility transistors due to the reduced phase space for carrier scattering in two-dimensionally confined systems. Experimental verification of this predicted phenomenon has, however, been elusive until recently when reduced exciton-exciton scattering rates were demonstrated in quantum wire arrays.[2] In this paper we experimentally explore one aspect of the problem, namely, the anisotropic scattering of long-wavelength acoustic phonons in quantum-wire arrays. Building on pioneering work in which surface-acoustic-wave (SAW) attenuation was used to measure the magnetoconductivity of a homogeneous two-dimensional electron gas (2DEG) (Refs. 3,4), we have investigated the anisotropic SAW scattering at $Al_xGa_{1-x}As$/GaAs quantum-wire arrays for the first time. This technique has many advantages. It is a contactless measurement and ideal for studying large arrays with good signal-to-noise ratio. SAW generation using interdigital transducers (IDT's) is also strongly directional and the long wavelengths used in our experiment (40 μm at 70 MHz) rule out possible diffraction effects. We show that the scattering rates are only strongly suppressed for SAWs propagating along the length of the wires, and then only for low electron concentrations in the narrowest structures investigated. Moreover, the scattering in this longitudinal direction at high carrier concentrations ($>8.1\times10^8$ m^{-1} for 500-nm wires, $>3.8\times10^8$ m^{-1} for 250-nm wires) rather surprisingly exceeds that of the unstructured 2DEG by a factor of 3. With the SAWs propagating perpendicular to the wires, when one naively expects *no* interaction classically, we observe strong oscillations in the transmitted intensity reflecting the magnetic depopulation of 1D subbands as described by a full quantum-mechanical description of the SAW-electron interaction.

The interaction between SAW's and 2D electrons has previously been described using a classical relaxation model,[3] where the attenuation per unit length Γ is a nonmonotonic function of the diagonal component of the conductivity tensor σ_{xx}

$$\Gamma = q\frac{K_{\rm eff}^2}{2}\frac{\sigma_{xx}/\sigma_M}{1+(\sigma_{xx}/\sigma_M)^2}, \tag{1}$$

where q is the SAW wave vector, $K_{\rm eff}$ is the effective piezoelectric coupling coefficient, and Γ has a maximum near a characteristic conductivity $\sigma_M(\approx 4\times10^{-7}\ \Omega^{-1})$. This classical approach, however, is only strictly valid when $ql\ll1$, where l is the electron elastic mean free path, and when $ql\gg1$ quantum-mechanical perturbation theory should be used.[5] Parallel to our wires, we estimate that $ql\sim1$ and neither a classical nor a quantum-mechanical approach is rigorously correct. However, we will show that both models predict negligibly small SAW scattering rates in this orientation.

Since σ_{xx} is clearly not defined perpendicular to the wires, our system demands a fully quantum-mechanical treatment in this orientation. Fermi's golden rule has been used to calculate the leading-order zero-temperature SAW-electron scattering rates. We assume that attenuation of the SAW signal is solely due to the absorption of single SAW quanta by the electronic system and neglect coupling between wires. The SAW energy quantum ($\hbar\omega\sim300$ meV) is negligible compared to the 1D subband spacing (1–2 meV), and the SAW wave vector ($q=1.6\times10^5$ m^{-1}) is very much smaller than a typical Fermi wave vector ($k_F\sim5\times10^8$ m^{-1}) except when a subband is almost depopulated. Consequently, only quasielastic intraband transitions need to be considered. The coupling between SAWs and electrons in GaAs is known to be predominantly via the piezoelectric interaction,[3] with the following Hamiltonian:[6]

$$H_{\rm piezo}=\frac{ee_{14}}{\varepsilon}\left(\frac{\hbar}{2\rho V\omega_q}\right)^{1/2}2i\sum_{\mathbf{q}}\frac{1}{q^2+q_0^2(B)}[\varepsilon_{\mathbf{q},x}q_yq_z+\varepsilon_{\mathbf{q},y}q_xq_z+\varepsilon_{\mathbf{q},z}q_xq_y](a_{\mathbf{q}}e^{i\mathbf{q}\cdot\mathbf{r}}+a_{\mathbf{a}}^{\dagger}e^{-i\mathbf{q}\cdot\mathbf{r}}), \tag{2}$$

where e_{14}, ρ, and ε are, respectively, the piezoelectric constant, mass density, and dielectric constant of GaAs, V is the sample volume, $\mathbf{q}$, and $\omega_{\mathbf{q}}$ are the SAW wave vector and frequency, $\varepsilon_{\mathbf{q}}$ is a unit polarization vector, a ($a^{\dagger}$) is the SAW annihilation (creation) operator, $q_0(B)$ is the magnetic-field-dependent inverse Thomas-Fermi screening length, and x, y, and z are the GaAs crystallographic axes.

With the SAW propagating in the [110] direction (x' coordinate) perpendicular to the wires, total momentum conservation is relaxed and only electron momentum along the wires must be conserved. In this case the scattering rate reduces to

$$\tau^{-1}=\frac{2\pi}{\hbar}\frac{e^2e_{14}^2}{\varepsilon^2}\left(\frac{\hbar}{2\rho\omega_{\mathbf{q}}}\right)\left(\frac{q^2}{q^2+q_0^2(B)}\right)^2 \times\sum_n |\langle\psi_n|e^{iqx'}|\psi_n\rangle|^2\frac{1}{\pi\hbar}\left(\frac{2m^*(B)}{[E_F-E_n(B)]}\right)^{1/2}, \quad (3)$$

where the assumption of a parabolic confinement potential allows one to retain the concept of one-dimensional subbands with modified effective masses [$m^*(B)$] and subband energies [$E_n(B)$] in finite magnetic fields.[7] The summation is over the n occupied 1D subbands and the matrix element, or ''form factor,'' is close to unity in all cases, since the SAW wavelength is very much longer than the width of the wires. Assuming that screening is weak in our system, we see that the B-dependent scattering rate is dominated by the total density of electronic states at the Fermi energy [last term of Eq. (3)]. This is plotted as a function of applied magnetic field in Fig. 1(b) for typical wire parameters after negation in order to model the transmitted SAW intensity. Note the strong oscillations as the Fermi energy drops through the singular density of states at a 1D subband edge. The two traces represent two different levels of Gaussian disorder broadening (σ_E) of the subband energies.

Applying the same quantum-mechanical approach with the SAW parallel to the wires requires total momentum conservation. This prohibits all SAW absorption except for the Umklapp process across the Fermi line when $|\mathbf{k}_F^n|=|\mathbf{q}|/2$. This yields the following expression for the scattering rate:

$$\tau^{-1}=\frac{2\pi}{\hbar}\frac{e^2e_{14}^2}{\varepsilon^2}\left(\frac{\hbar}{2\rho\omega_{\mathbf{q}}}\right)\left(\frac{q^2}{q^2+q_0^2(B)}\right)^2\frac{2m^*(B)}{\pi\hbar^2q} \quad \text{when } |\mathbf{q}|=2|\mathbf{k}_F| \quad (4)$$

and zero otherwise. We see that scattering is now only allowed for a few *discrete* magnetic fields just before a subband depopulates, and once inhomogeneous broadening is taken into account we would not expect to be able to resolve this. The last term in Eq. (3) (the dominant contribution to the density of states at the Fermi energy when $|\mathbf{q}|=2|\mathbf{k}_F|$) is plotted negated as a function of magnetic field in Fig. 3(b) for the same wire parameters and disorder broadening as before and assuming that the SAW power is uniformly distributed in the range $f=70\pm2.5$ MHz due to our pulsed measurement mode. Note that although oscillatory attenuation is predicted, it is *four* orders of magnitude weaker than in the other orientation. Our estimate of $\sigma_{xx}\sim10^{-2}\ \Omega^{-1}$ in this orientation is five orders of magnitude greater than σ_M and hence negligible SAW scattering rates are also predicted in the classical picture [Eq. (1)]. This situation would not change significantly upon application of a magnetic field.

Measurements were made on arrays of quantum wires fabricated from an $Al_xGa_{1-x}As/GaAs$ heterostructure, grown by molecular-beam epitaxy on a semi-insulating (001) GaAs substrate, with an unstructured carrier concentration of 2.1×10^{15} m^{-2} and a mobility of 60 m^2/V s at 4.2 K. Holographic lithography and reactive ion etching with $SiCl_4$ were used to pattern the samples yielding arrays of wires of geometrical width of either 500 or 250 nm, with periods of 1000 and 500 nm, respectively. The wires were orientated parallel to the [$\bar{1}$10] axis. To minimize edge depletion, the etch depth ($\sim$85 nm) was less than the depth of the 2DEG below the surface (105 nm). A final wet mesa etch left a 3×3-mm square of approximately 3000 (6000) nanostructures in the center of each sample. IDT's were realized on the exposed edges of the substrate by thermal evaporation of Cr/Au fingers. The center-to-center spacing of the fingers in each transducer was 20 μm, yielding a broad SAW resonance of about 70 ± 5 MHz. Measurements were made by exciting 0.4-μs-long SAW pulses, at a repetition rate of 250 kHz, from one transducer and receiving them at the opposite transducer. The SAW's propagate either in the [110] or [$\bar{1}$10] direction, parallel or perpendicular to the wires, which have the strongest piezoelectric coupling coefficient[3] and carry a longitudinal electric field. The SAW power at the sample ($\sim$0.1 μW) was reduced to well below the level where there was any evidence of heating of the electron gas. Our detection system is based on an eight-tap digital delay line and measures changes in both the amplitude and phase (or velocity), to better than one part in 10^4 and one part in 10^5, respectively. Measurements were performed in a 10 T liquid-helium cryostat at 1.3 K with the magnetic field perpendicular to the plane of the samples.

Figures 1(a) and 1(c) show transmitted SAW intensity as a function of applied magnetic field for SAW propagation perpendicular to the 500-nm and 250-nm quantum wires, respectively. Persistent photoconductivity was used to increase the electron concentration in the samples (100-ms-long 50-mA pulses from an infrared LED), and successive traces on both figures have been offset by -10 units on the y axis for clarity. In all cases, velocity shift data mirrors the intensity data, and Fig. 1(a) also shows SAW velocity shift for the highest-illumination case. Each trace has been labeled with a calculated 1D electron concentration (see below). In Fig. 1(c) the traces are also labeled by the total illumination time in seconds, since too few magneto-oscillations were observed in the zero-illumination case for it to be possible to calculate an electron concentration. The SAW intensity oscillations in both sizes of wires are attributed to the magnetic depopulation of 1D subbands, with the minima corresponding to the peak in the electronic density of states when the Fermi energy lies near a subband edge. The good agreement between the magnetic-field positions of the minima in $-g(E_F)$ [Fig. 1(b)] and those of the equivalent SAW intensity [the third trace in Fig. 1(a)] suggests that SAW absorption is, as predicted quantum mechanically, predominantly proportional to the density of states at the Fermi energy. However, the failure of the simulation to faithfully reproduce the measured line shapes of the wide wires near depopulation, even after the inclusion of substantial disorder broadening (e.g.,

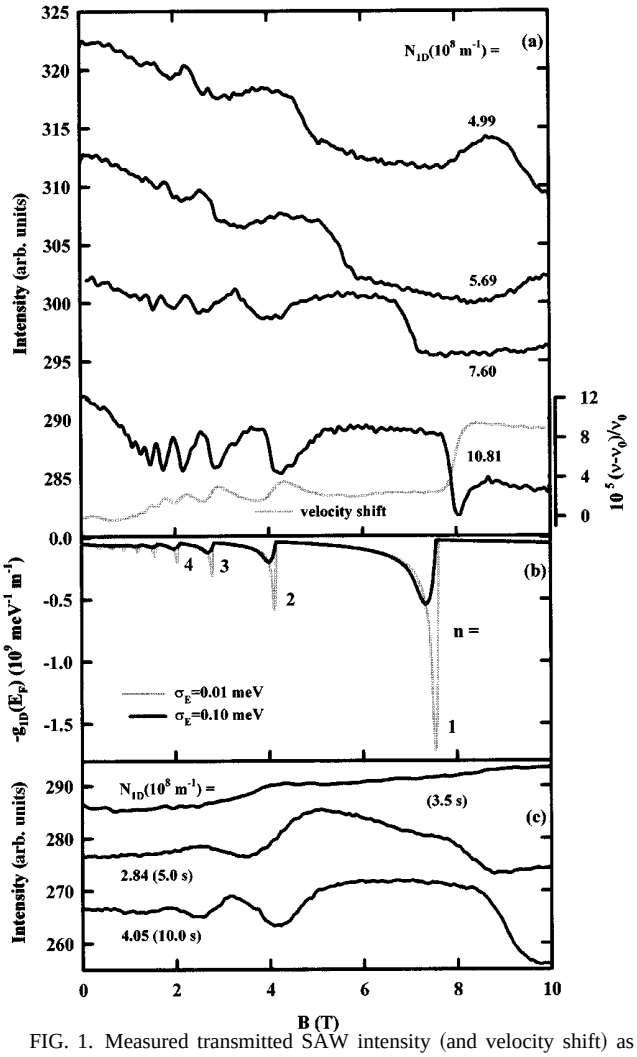

FIG. 1. Measured transmitted SAW intensity (and velocity shift) as a function of magnetic field for (a) 500-nm and (c) 250-nm quantum wires, with the SAW's propagating perpendicular to the wires. The calculated electronic density of states at the Fermi energy is plotted negated in (b) for $N_{1D}=7.6\times10^8$ m^{-1} and $\frac{1}{2}\hbar\omega_0=0.85$ meV.

$\sigma_E=0.1$ meV), implies that the screening of the SAW-electron interaction $[q_0(B)]$ must play a significant role even in 1D. The line shapes in the narrow wires, Fig. 1(c), agree rather better, as one would expect, since the more confined wave-function states will respond more weakly to the linear applied SAW electric field and hence screening will be less important. We also note that the $n=1$ minimum, and to some extent the higher minima, in the lowest trace of Fig. 1(a) are much more clearly defined than at lower illumination levels, suggesting that static screening of disorder is considerably more effective at very large electron concentrations, as one would expect.

Assuming parabolic electrostatic confinement, the following nonlinear relationship can be derived for the magnetic field when the $(n+1)$th subband has just been depopulated:[7]

$$N_{1D}=\frac{2}{\pi}(2m^*/\hbar)^{1/2}\left\{\left[\left(\frac{eB}{m^*}\right)^2+\omega_0^2\right]^{3/4}\Big/\ \omega_0\right\}\sum_{j=1}^{n}\sqrt{j}, \qquad (5)$$

where m^* is the normal effective mass, N_{1D} is the 1D electron concentration, and ω_0 is a characteristic frequency defining the electrostatic confinement. N_{1D} and the characteristic confinement energy $(1/2\hbar\omega_0)$ can be obtained from linear plots of B^2 versus $(\Sigma_{j=1}^{n}\sqrt{j})^{-4/3}$ at the SAW intensity minima (see inset of Fig. 2). These are then plotted in Fig. 2 for a range of illumination levels in both 500-nm and 250-nm wires. The confinement energy of the narrow wires is approximately a factor of 2 larger than for the wide wires, in broad agreement with our assumption of parabolic confinement. The characteristic confinement energy decreases with increasing carrier concentration in both cases. This is expected due to self-consistent screening of the potential,[8] with a more rapid change visible in the 250-nm wires, which have less occupied 1D subbands. The effective electronic widths of the wires also increase with increasing electron concentration and are smaller than the geometric widths due to sidewall depletion, which is expected to be $\sim$100 nm at each edge.

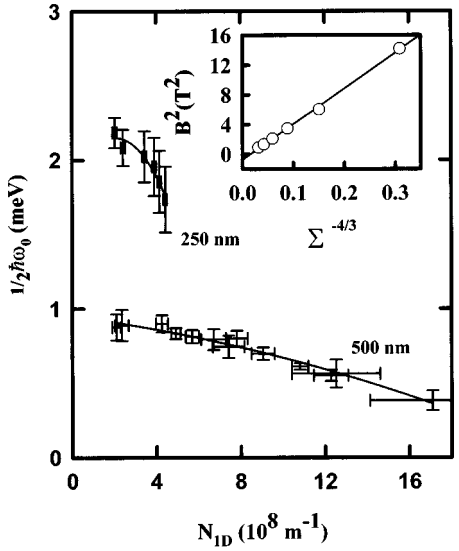

FIG. 2. Plot of characteristic confinement energies as a function of 1D electron concentration for both 500-nm and 250-nm quantum wires. The inset shows a typical linear fit to B^2 vs $(\Sigma_{j=1}^{n}\sqrt{j})^{-4/3}$.

Figures 3(a) and 3(c) show transmitted SAW intensity as a function of magnetic field with the SAW's propagating parallel to the wires (the same array was used for both the perpendicular and parallel measurements). Note that the traces have *not* been offset in this figure. The traces are labeled with N_{1D} values that have been established from consecutive measurements with the SAW's perpendicular to the wires. We see no evidence for Umklapp scattering near fields corresponding to subband depopulation as depicted in Fig. 3(b). This is to be expected, due to the relative weakness of this channel. In the wide wires [Fig. 3(a)], an initial increase in electron concentration with illumination actually leads to an increase in the measured SAW intensity. This may be due to a reduction in disorder coupling (disorder relaxes the momentum conservation rules) as N_{1D} is increased and the disorder is screened. Additional illumination, however, leads to a strong reduction in SAW intensity. In the narrow wires there is no significant change in SAW intensity from the zero-illumination case [the dotted line in Fig. 3(c)] until the saturation electron concentration is almost reached, when the SAW intensity drops rapidly. The much more confined states in the narrow wires make them less sensitive to disorder and this is probably why we measure no significant disorder cou-

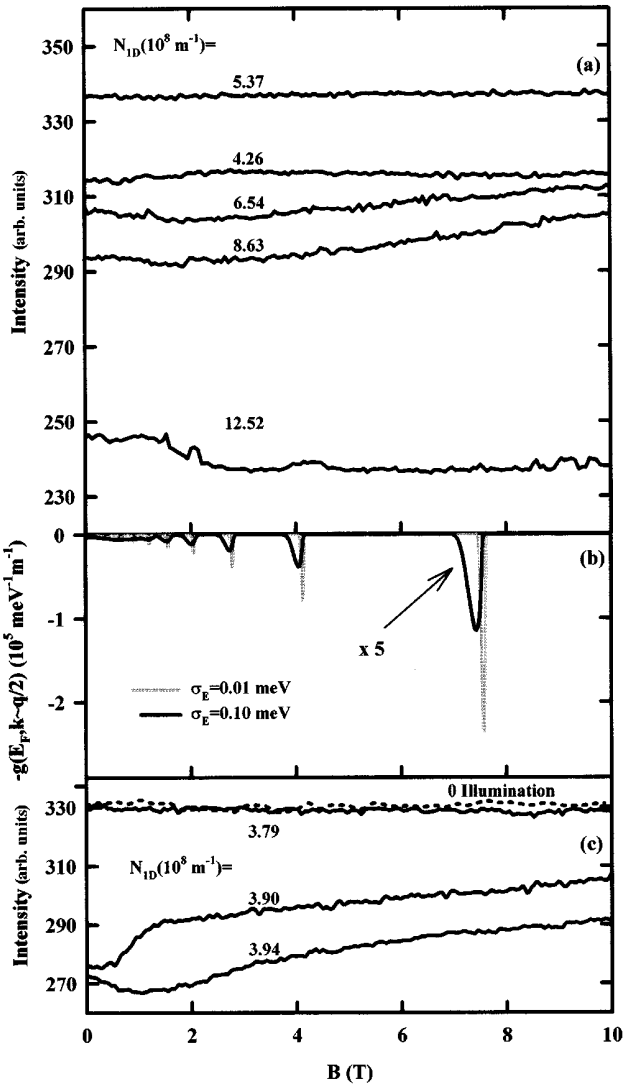

FIG. 3. Measured transmitted SAW intensity as a function of magnetic field for (a) 500-nm and (c) 250-nm quantum wires, with the SAW's propagating parallel to the wires. The contribution of the highest subband to the electronic density of states at the Fermi energy when $|\mathbf{k}_F^n| = |\mathbf{q}|/2$ is plotted negated in (b) for $N_{1D} = 7.6 \times 10^8$ m^{-1} and $\frac{1}{2}\hbar\omega_0 = 0.85$ meV.

pling here. At high electron concentrations the transmitted SAW intensity in both cases seems to show broad magnetic-field-dependent resonances superimposed on a gently varying background. Parallel conduction in the modulation-doped $Al_xGa_{1-x}As$ layer is one possible explanation for the surprisingly large SAW absorption at high illumination levels. However, the fall in intensity from the low- to high-illumination traces corresponds to an attenuation of ~ 3.5 dB/cm, which is considerably larger than the maximum possible predicted of ~ 1.1 dB/cm for an unstructured 2DEG (when the conductivity changes from zero to σ_M), calculated using the classical relaxation model. In addition, this strong attenuation is absent in the perpendicular direction (n^+ $Al_xGa_{1-x}As$ is highly disordered and would not be expected to show significant confinement effects), and these two facts indicate that parallel conduction is not responsible. SAW's have been used previously to study edge magnetoplasmons.[9] Since the frequency of these diverges as the applied magnetic field tends to zero, they cannot alone explain our data, but the excitation of other plasmonic modes must be considered. Recent work by Sun, Liu, and Yu[10] has calculated the collective excitations of arrays of parallel quantum-well wires. In the limit of our experiment, they predict a 2D-plasmon-like acoustic intrasubband excitation in the direction of the wires, which depends on the mean two-dimensional electron density, N_{2D}; ($\omega_{pl} \approx \sqrt{[(N_{2D}e^2)/(2m^*\varepsilon)]q}$). This dispersion curve is, however, three orders of magnitude too steep to allow the SAW to make energy- and momentum-conserving transitions. We note, however, that the theory neglects interactions between 1D subbands and we speculate that this could strongly influence the plasmon dispersion and possibly allow the SAW's to couple.

In conclusion, we have observed strongly anisotropic surface acoustic-wave scattering from quantum-wire arrays. The data are in fair agreement with our theoretical calculations in the perpendicular direction, but surprisingly show a sharp increase in attenuation at high electron concentrations in the longitudinal direction. We speculate that this could possibly be due to excitation of intrasubband 2D plasmonlike modes.

We acknowledge the support of the Royal Society and the Engineering and Physical Sciences Research Council of the U.K. (Grant No. GR/K69742) and thank J. C. Inkson for fruitful discussions.

[1] H. Sakaki, in *Springer Series in Solid State Sciences*, edited by F. Kuchar, H. Heinrich, and G. Bauer (Springer-Verlag, Berlin, 1990), Vol. 97, p. 2.
[2] M. Oestreich, W. W. Rühle, H. Lage, D. Heitmann, and K. Ploog, Phys. Rev. Lett. **70**, 1682 (1993).
[3] A. Wixforth, J. Scriba, M. Wassermeier, J. P. Kotthaus, G. Weimann, and W. Schlapp, Phys. Rev. B **40**, 7874 (1989).
[4] R. L. Willet, K. W. West, and L. N. Pfeiffer, Phys. Rev. Lett. **75**, 2988 (1995).
[5] J. H. McFee, in *Physical Acoustics*, edited by W. Mason (Academic, New York, 1966), Vol. 4A, pp. 1–47.
[6] B. K. Ridley, *Quantum Processes in Semiconductors* (Clarendon, Oxford, 1982).
[7] K.-F. Berggren, G. Roos, and H. van Houten, Phys. Rev. B **37**, 10 118 (1988).
[8] S. E. Laux, D. J. Frank, and F. Stern, Surf. Sci. **196**, 101 (1988).
[9] P. Hawker, P. F. Lenne, M. Tonouchi, V. W. Rampton, C. J. Mellor, and M. Henini, Physica B **194-196**, 419 (1994).
[10] H. Sun, Y. L. Liu, and K. W. Yu, J. Phys. Condens. Matter **7**, 3539 (1995).